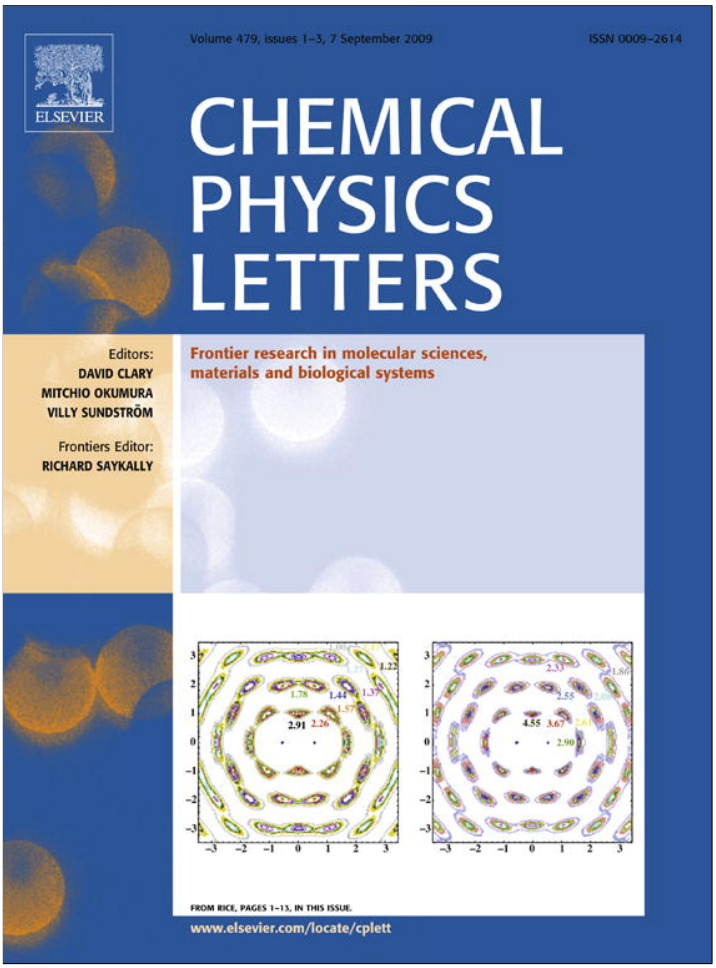

Chemical Physics Letters 479 (2009) 140–143

Contents lists available at ScienceDirect

Chemical Physics Letters

journal homepage: www.elsevier.com/locate/cplett

Wavelength-dependent electron–phonon coupling in impurity glasses

Margus Rätsep [a], Mihkel Pajusalu [a], Arvi Freiberg [a,b,*]

[a] Institute of Physics, University of Tartu, Riia 142, 51014 Tartu, Estonia
[b] Institute of Molecular and Cell Biology, University of Tartu, Riia 23, 51010 Tartu, Estonia

ARTICLE INFO

Article history:
Received 30 June 2009
In final form 29 July 2009
Available online 3 August 2009

ABSTRACT

By applying an advanced hole-burning fluorescence line-narrowing technique, an unexpectedly strong (several-fold) increase of the electron–phonon coupling strength on excitation wavelength through the inhomogenously broadened absorption origin band was first observed for low-temperature organic glass samples doped with biologically relevant chlorin and chlorophyll *a* molecules. The dependence, which suggests a direct correlation between solvent shift and the electron–phonon coupling, demonstrates great sensitivity of the zero-phonon transitions localized on single chromophores as optical probes of the structure and dynamics of local subnanoscopic environments.

1. Introduction

Impurity spectroscopy is a well-established branch of condensed-matter physics with multiple applications [1–4]. Nevertheless, certain aspects of the guest–host spectroscopy remain poorly studied/understood, partially due to experimental difficulties. One of these open questions is the focus of this Letter. The difference in coupling between the electrons in the excited state and that between the electrons in the ground state and the nuclear vibrations, including local intramolecular and extended matrix phonons, determines the characteristic (homogeneous) shape of the impurity spectra. It also governs the dynamic properties of the system. The homogeneous spectrum at low temperatures consists of a narrow pure electronic (0–0) zero-phonon line (ZPL) with a broad phonon wing attached to it and the vibrational replicas of the 0–0-group. Static variations of the guest–host interactions lead to inhomogeneous broadening and to loss of selectivity of the spectra, significantly impeding most applications. Typical spread (defined as full width at half maximum, fwhm) of the inhomogeneous distribution of the guests' 0–0 levels (IDF) in organic glasses is 60–500 cm^{-1} [5]. It 10^3–10^4 times exceeds the average lifetime-broadened width of the ZPL-s at low temperatures. Because of an overlap of ZPL-s and phonon wings of different impurities in inhomogeneously broadened spectra, the experimental data about the dependence of the electron–phonon and/or electron–vibrational interaction strengths on excitation wavelength within the IDF have been both scarce and inconclusive [6–8]. Hence, this dependence is commonly ignored. A difference fluorescence-line-narrowing spectroscopy (ΔFLN) [6,9,10] based on persistent spectral hole-burning (HB) provides unique opportunities to study optical spectra of selected subgroups of chromophores in disordered systems such as low-temperature glasses and proteins with high resolution. Recent ΔFLN measurements on various plant and bacterial antenna complexes (FMO [10], CP29 [11], LH1, and LH2 [12]) discovered a dependence of the electron–phonon coupling strength on the excitation wavelength. The origin of this dependence, however, remains obscure due to the overwhelming complexity of the chromophores in protein environments. Therefore, in this work, much simpler samples of chlorophyll *a* as well as of its metal-free derivative chlorin (7,8-dihydroporphin) in a glassy matrix of 1-propanol have been examined. A strong wavelength dependence of the electron–phonon coupling strength was unambiguously established.

2. Method

The dimensionless parameter, S, which describes the total linear electron–phonon coupling strength is called the Huang–Rhys factor [13]. Its physical meaning is the average number of phonons that accompany a particular electronic transition. By combining HB with fluorescence line narrowing (FLN), the ΔFLN spectroscopy distinctively allows determining the S values over the full extent of the IDF [9,10]. Experimentally the ΔFLN spectra are obtained as difference spectra between two FLN spectra, one obtained before and the second, after the intermediate HB stage. Within the Franck–Condon approximation the ΔFLN spectrum in short-burn-time limit is calculated as [14,15]:

$$\Delta FLN(\nu) \propto \sum_{R,P=0}^{\infty} \left(S^R \frac{e^{-S}}{R!}\right)\left(S^P \frac{e^{-S}}{P!}\right) \int d\Omega N(\Omega - \nu_C) I_R(\nu - \Omega + R\nu_m) \times I_p(\nu_E - \Omega - P\nu_m). \quad (1)$$

* Corresponding author. Address: Institute of Physics, University of Tartu, Riia 142, 51014 Tartu, Estonia. Fax: +372 738 3033.
E-mail address: arvi.freiberg@ut.ee (A. Freiberg).

0009-2614/$ - see front matter © 2009 Elsevier B.V. All rights reserved.
doi:10.1016/j.cplett.2009.07.094

In Eq. (1), $N(\Omega - \nu_C)$ is the previously introduced IDF of the impurity transition energies centered at ν_C, and ν_E is the excitation frequency. The ZPL peaking at ν_E corresponds to all transitions with $R, P = 0$, while all other transitions constitute the phonon wing. The l_R-terms with $R = 1, 2, \ldots$ relate to the one-phonon and multi-phonon ($R \geqslant 2$) transitions. The l_1 term is commonly called the spectral density function. For comparison with the experiment, the calculated ΔFLN spectrum should be multiplied by ν^3 to account for the frequency dependence of the fluorescence.

Selective excitation was carried out using a Spectra Physics model 375 dye laser with a linewidth <0.5 cm^{-1}. The spectra were recorded with a 0.3 m spectrograph equipped with a CCD camera (both Andor Technology). All the experiments were performed in a helium bath cryostat, where the samples were kept just above the level of liquid helium at 4.5 ± 0.2 K. The Huang–Rhys factors were calculated according to

$$\exp(-S) = \frac{I_{ZPL}}{I_{ZPL} + I_{PSB}} = \alpha, \quad (2)$$

where I_{ZPL} and I_{PSB} are the integral intensities of the ZPL and of the real phonon sideband (PSB), respectively, and α is the familiar Debye–Waller factor related to the zero-phonon transition probability. The I_{PSB} term requires an explanation. Besides resonantly excited real-PSB an experimental phonon spectrum contains parts called pseudo- and multi-PSB, which originate from non-resonant excitation of the chromophores through their phonon sidebands. Owing to these extra contributions the relative (with respect to I_{ZPL}) PSB intensity in the FLN spectrum appears larger than it is in the actual homogeneous spectrum. It also causes an apparent dependence of the spectral shape on excitation wavelength [16]. Therefore, to obtain the correct S value, the experimental phonon spectrum must be disentangled into its various components and only the real-PSB must be used in Eq. (2). This crucial procedure is described in detail in [9,15].

3. Results and discussion

The conventional (low-resolution) absorption and fluorescence emission spectra of chlorin in 1-propanol are shown in Fig. 1. The spectra with partially resolved vibronic structure well illustrate the mirror symmetry rule for the conjugate $S_1 \leftrightarrow S_0$ electronic transitions. The almost perfect overlap of the inhomogenously broadened spectral origins (no Stokes shift) implies very weak electron–phonon coupling between the impurity molecule and the surrounding glass. It also evidences lack of any significant excited state energy transfer during the excited state lifetime at the applied concentration of $\sim 1 \times 10^{-5}$ M of the chlorin molecules. The ΔFLN spectrum with much improved resolution is shown as a green line. It consist from a sharp ZPL line at the excitation laser wavelength overshooting the intensity scale of the figure, a low-frequency phonon wing located to the red of the ZPL, and several vibronic replicas of the origin band red-shifted by the chlorin vibrational frequencies. The inset of Fig. 1 shows an expanded view of the absorption origin together with series of spectral holes burned into it. Each hole is obtained using the same nonsaturating (see inset of Fig. 3 below) burn laser fluence of 12 mJ/cm^2. The distribution of the hole depths defines the IDF, as shown in Fig. 3.

As follows, we shall focus on the phonon wing of the ZPL in the ΔFLN spectrum, which reflects the coupling of the $S_1 \leftrightarrow S_0$ electronic transition in chlorin to a continuum of delocalized vibrations of the surrounding matrix. Fig. 2a represents the FLN and ΔFLN spectra in the phonon wing region using 631.9-nm excitation. The top curve is the initial FLN spectrum, recorded before intentional hole-burning of the sample (the pre-burn spectrum). The blue curve below is the post-burn FLN spectrum, obtained after burning with exposure of 92 mJ/cm^2. The difference between the pre- and post-burn spectra, the ΔFLN spectrum, is presented with the bottom red curve. The same spectrum is displayed in full intensity scale in the inset. The real-PSB contribution to the phonon spectrum, recovered by model calculations, is indicated in Fig. 2b by a bold green line. For modeling, an empirical shape of the spectral density function is used, being composed from a Gaussian low frequency and a Lorentzian high frequency halves [14]. As seen, at this specific excitation wavelength the real-PSB comprises a minor part from the recorded phonon wing. The rest of the wing is due to non-resonantly excited pseudo- and multi-PSB contributions. Blue and brown lines show them, respectively. It is of notice that in FLN spectra the ZPL is usually strongly contaminated with scattering from the excitation laser, preventing a proper determination of its intensity, I_{ZPL}. Thanks to the subtraction inherent to the ΔFLN

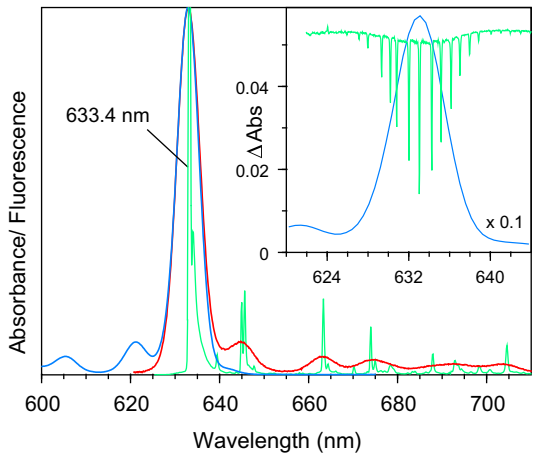

Fig. 1. Conventional absorption (blue) and fluorescence emission (red, excited at around 470 nm) spectra of chlorin-doped 1-propanol at 4.5 K. The ΔFLN spectrum (green, measured with resolution of ~8 cm^{-1}) at 633.4-nm excitation is obtained with burn fluence of 92 mJ/cm^2. There are no detectable vibrational modes beyond the spectral range presented. The zero-phonon line is cut off at 12% of its peak intensity value. The inset demonstrates series of spectral holes (green) burned into the 0–0-absorption origin band (blue, multiplied by 0.1). (For interpretation of the references to color in this figure legend, the reader is referred to the web version of this article.)

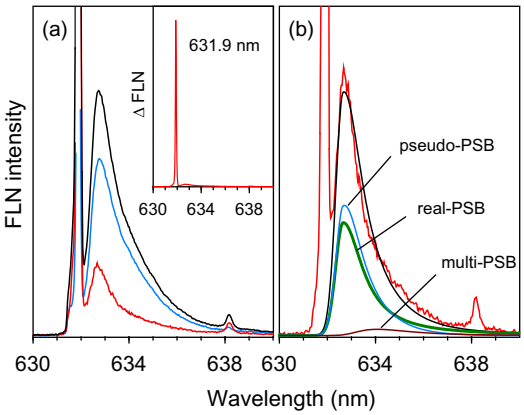

Fig. 2. (a) Expanded view of the selectively excited FLN (two top curves, recorded with the low fluence of 2 mJ/cm^2) and ΔFLN (lower red curve, hole-burning fluence of 92 mJ/cm^2) spectra in the 0–0 origin range of the chlorin-doped 1-propanol glass. The inset shows the same ΔFLN spectrum with full ZPL intensity at 2 cm^{-1} spectral resolution. (b) Simulations of the ΔFLN spectrum from part (a) (red noisy curve). The model ΔFLN spectrum (black curve) is calculated using $S = 0.049$, peak phonon frequency of $w = 19$ cm^{-1}, and fwhm of the Gaussian and the Lorentzian distributions of 18 cm^{-1} and 48 cm^{-1}, respectively. (For interpretation of the references to color in this figure legend, the reader is referred to the web version of this article.)

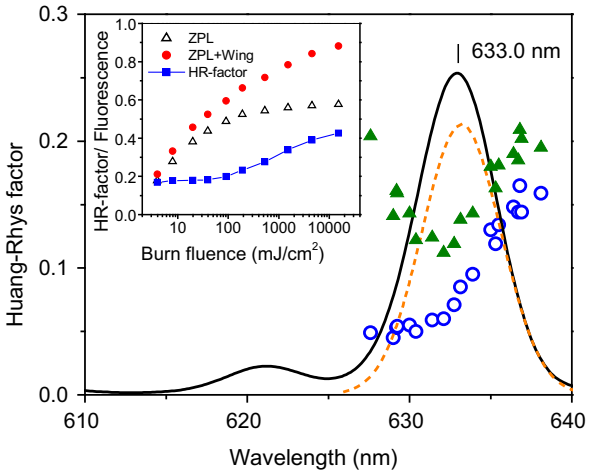

Fig. 3. Wavelength dependence of the apparent electron–phonon coupling strength (green triangles) and the actual S (blue rings) recovered from spectral simulations for the chlorin-doped 1-propanol on the background of the absorption spectrum (continuous curve) and IDF (dashed curve). The IDF of 5.7 nm (142 ± 10 cm^{-1}) fwhm peaks at 633.3 ± 0.2 nm. The inset demonstrates changing integral intensity of the ΔFLN spectrum (dots) and its ZPL component (triangles) with burn fluence measured at 633.7 nm. The corresponding apparent (before correction for the real-PSB intensity) Huang–Rhys factor values are plotted with squares. (For interpretation of the references to color in this figure legend, the reader is referred to the web version of this article.)

technique, however, the latter spectra are virtually free from the scattering artifact [10,11]. The ZPL saturation errors, characteristic to hole-burning methods were avoided using sufficiently low burn fluencies (<100 mJ/cm^2), according to the inset of Fig. 3.

Figs. 3 and 5 present the main experimental findings of this work, i.e., excitation wavelength dependences of the electron–phonon coupling strength for chlorin and chlorophyll *a* impurities, respectively, obtained with low burn fluence. Both apparent (uncorrected for the real-PSB) and corrected S-factors are presented. As seen, the apparent S-values significantly exceed the actual electron–phonon coupling strength. The correction factors decrease toward longer wavelengths because of relatively smaller amount of non-resonantly (through PSB) excited chromophores [16]. The results for chlorin (Fig. 3) show a more than threefold *increase* of S over ~10 nm spectral range, from 0.05 to 0.16 between 627.6 and 638.1 nm. The increase is rather slow at the blue side of the absorption contour but accelerates rapidly towards longer wavelengths. The corresponding *decrease* of the Debye–Waller factor representing the zero-phonon transition probability is from 0.95 to 0.85. The increase of S is generally accompanied with broadening of the Lorentzian part of the spectral density function from ~34 cm^{-1} at 629.2 nm to ~66 cm^{-1} at 636 nm (Fig. 4), the fwhm of the Gaussian component staying around 18 cm^{-1} all the way. At the same time the peak of spectral density function shifts from around 18 to 21 cm^{-1}.

The results for chlorophyll *a*, which are truncated from the high-energy side due to overlap with the Q_x electronic state, are similar (Fig. 5). The Huang–Rhys factors increase quasi-linearly from 0.17 to 0.49 between 669.3 and 693.3 nm, while the Debye–Waller factors decrease from 0.84 to 0.61. In contrast, no wavelength dependence of the vibronic Huang–Rhys factors, S_j, was observed. The total Huang–Rhys factor, $\sum_j S_j$, for the chlorin and chlorophyll *a* vibrations between 150 and 1600 cm^{-1} equals to 0.28 ± 0.03 and 0.53 ± 0.07, respectively. The individual S_j values were calculated according to $\exp(-S_j) = I_{0-0}/(I_{0-0} + I_j)$, where I_j is the integral intensity of the particular vibronic line, and I_{0-0} is the total intensity of the 0–0 band including its phonon wing.

Hole-burning [14] and single molecule [17] spectroscopies at selected wavelengths have previously been applied for determination of the Huang–Rhys and/or Debye–Waller factors. While the latter technique suffers from low signal, the reliability of HB is limited by the narrow spectral width of IDF deforming the shape of the pseudo-PSB [9]. Also, the HB photoproducts tend to interfere with the real-PSB, being on the high-energy side from ZPL in HB spectra. These experimental complications explain the virtual lack of any wavelength dependence of the electron–phonon coupling strength in earlier studies. Observing for the first time such a strong dependence is nonetheless surprising. Possible sources of error, such as interference with energy transfer or the hole-burning products should, therefore, be critically considered. Energy transfer, if present, would result in an opposite dependence, i.e., decrease of the coupling strength with the excitation wavelength. It is also excluded by the above very small Stokes shift. As to the second cause, chlorin and chlorophyll *a* distinguish from each other by the hole-burning mechanism. In the photochromic free-base chlorin, efficient photo-induced turning of the central proton pair by 90° takes

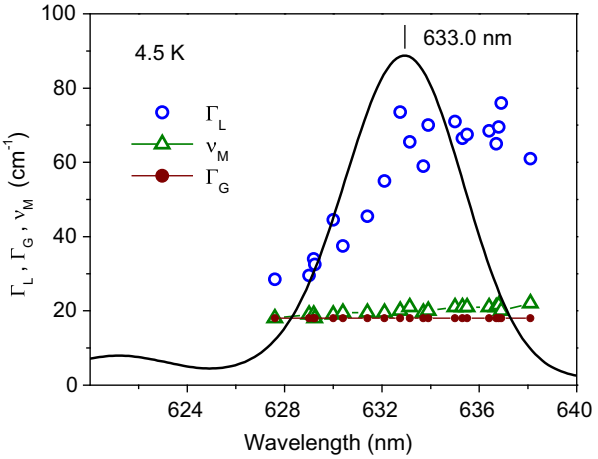

Fig. 4. Wavelength dependence of the spectral density function in chlorin-doped 1-propanol. The Lorentzian width, Γ_L (blue rings), the Gaussian width, Γ_G (brown dots), and the peak frequency, ν_M (green triangles), are shown on the background of the absorption spectrum. (For interpretation of the references to color in this figure legend, the reader is referred to the web version of this article.)

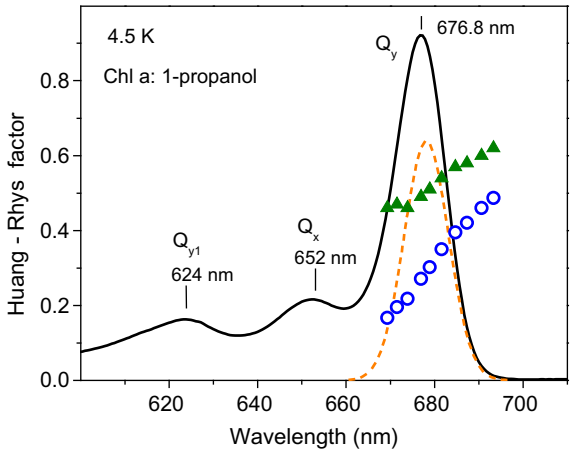

Fig. 5. Wavelength dependence of the apparent electron–phonon coupling strength (green triangles) and the actual S (blue rings) recovered from spectral simulations for chlorophyll *a*-doped 1-propanol on the background of the absorption spectrum (continuous curve) and IDF (dashed curve). The IDF of 12.7 nm (280 ± 40 cm^{-1}) fwhm peaks at 678.2 ± 0.5 nm. Q_y and Q_x in the absorption spectrum refer to the two chlorophyll *a* electronic transitions. (For interpretation of the references to color in this figure legend, the reader is referred to the web version of this article.)

place, which results in ~60 nm blue shift of the hole-burning product absorption spectra, well outside the origin absorption band [18]. In the so-called non-photochemical HB mechanism, related to the more photostable chlorophyll *a*, the impurity molecule just senses subtle light-induced environmental changes. Hence, the 'photoproduct' spectra distribute around the chlorophyll *a* origin absorption band. The fact that very similar results were obtained for the two impurity molecules with totally different HB mechanisms practically excludes confusing of the data with the HB products. The regular burn fluence dependence of the spectral parameters also rules out any artifact due to the dependence of the size or nature of the burned subensemble on the wavelength of the burning radiation. In fact, the Huang–Rhys factor is independent on exposure as far as saturation is avoided (Fig. 3).

Qualitative explanation of the observations requires a direct correlation of the electron–phonon coupling strength with the 0–0-transition energy. Strong color effects in amorphous host materials due to correlated guest–host interactions are previously found in pressure tuning and Stark HB spectroscopy [19]. Although a microscopic theory of these phenomena is still to be developed, a rise of the Huang–Rhys factor with increasing wavelength can be explained by a simple phenomenological approach using the Lennard–Jones 6–12 potentials, which represent the exchange repulsion and London (dispersion) forces with different nuclear configurations in the ground and excited states [20]. A particularly strong increase of the Huang–Rhys factors is expected if the equilibrium distance of the excited state potential is larger than the ground state one. The present new and unexpected result, a strong correlation between the red shift of the electronic 0–0-transition energy of the chromophore with the value of the Huang–Rhys factor, will hopefully promote further understanding of fundamental interactions in sensitized amorphous solids, including biological pigment–protein complexes.

Acknowledgement

Financial support from the Estonian Science Foundation Grant No. 7002 is gratefully acknowledged.

References

[1] F. Seitz, D. Turnbull, Solid State Physics, vol. 8, Academic Press, New York, 1959.
[2] K.K. Rebane, Impurity Spectra of Solids, Plenum Press, New York, 1970.
[3] A.V. Fedorov, V.A. Kremerman, A.I. Ryskin, Phys. Rep. 248 (1994) 369.
[4] I.S. Osad'ko, Phys. Rep. 206 (1991) 43.
[5] T. Reinot, V. Zazubovich, J.M. Hayes, G.J. Small, J. Phys. Chem. B 105 (2001) 5083.
[6] J. Wolf, K.-Y. Law, A.B. Myers, J. Phys. Chem. 100 (1996) 11870.
[7] N. Verdal, A.M. Kelley, J. Chem. Phys. 117 (2002) 8996.
[8] A. Freiberg, L. Rebane, in: O. Sild, K. Haller (Eds.), Zero-phonon Lines and Spectral Hole Burning in Spectroscopy and Photochemistry, Springer Verlag, Berlin, Heidelberg, 1988, p. 55.
[9] M. Rätsep, A. Freiberg, Chem. Phys. Lett. 377 (2003) 371.
[10] M. Rätsep, A. Freiberg, J. Lumin. 127 (2007) 251.
[11] M. Rätsep, J. Pieper, K.-D. Irrgang, A. Freiberg, J. Phys. Chem. B 112 (2008) 110.
[12] A. Freiberg, M. Rätsep, K. Timpmann, G. Trinkunas, Chem. Phys. 357 (2009) 102.
[13] M. Lax, J. Chem. Phys. 20 (1952) 1752.
[14] J.M. Hayes, P.A. Lyle, G.J. Small, J. Phys. Chem. 98 (1994) 7337.
[15] J. Pieper, J. Voigt, G. Renger, G.J. Small, Chem. Phys. Lett. 310 (1999) 296.
[16] J. Kikas, Chem. Phys. Lett. 57 (1978) 511.
[17] C. Hofmann, H. Michel, M. van Heel, J. Köhler, Phys. Rev. Lett. 94 (2005) 195501.
[18] S. Völker, R.M. Macfarlane, J.H. van der Waals, Chem. Phys. Lett. 58 (1978) 8.
[19] M. Köhler, J. Friedrich, J. Fidy, BBA 1386 (1998) 255.
[20] I. Renge, J. Lumin. 128 (2008) 413.